

OBSERVATION: BRIEF RESEARCH REPORT

Histopathologic Changes and SARS-CoV-2 Immunostaining in the Lung of a Patient With COVID-19

Background: Although many studies have demonstrated the epidemiologic characteristics of SARS-CoV-2 disease (COVID-19), details of pathologic changes in the lung are still lacking.

Objective: To describe the histopathologic changes in the lung of a patient with COVID-19.

Case Report: A 72-year-old man with a history of diabetes and hypertension presented with fever and cough. His throat and pharyngeal swabs were positive for SARS-CoV-2 by day 6 after the initial symptoms. Rapidly progressive respiratory failure required endotracheal intubation and mechanical ventilation 1 week after presentation.

Lung tissue was obtained by transthoracic 14-gauge needle biopsy from the left upper anterior segment (Figure 1, A, arrow), left upper lingular segment (Figure 1, B, arrow), and left lower lobe (Figure 1, C, arrow), coinciding with ground-glass opacities on chest computed tomography (CT). Two throat swab samples were collected from the tonsils and posterior pharyngeal wall.

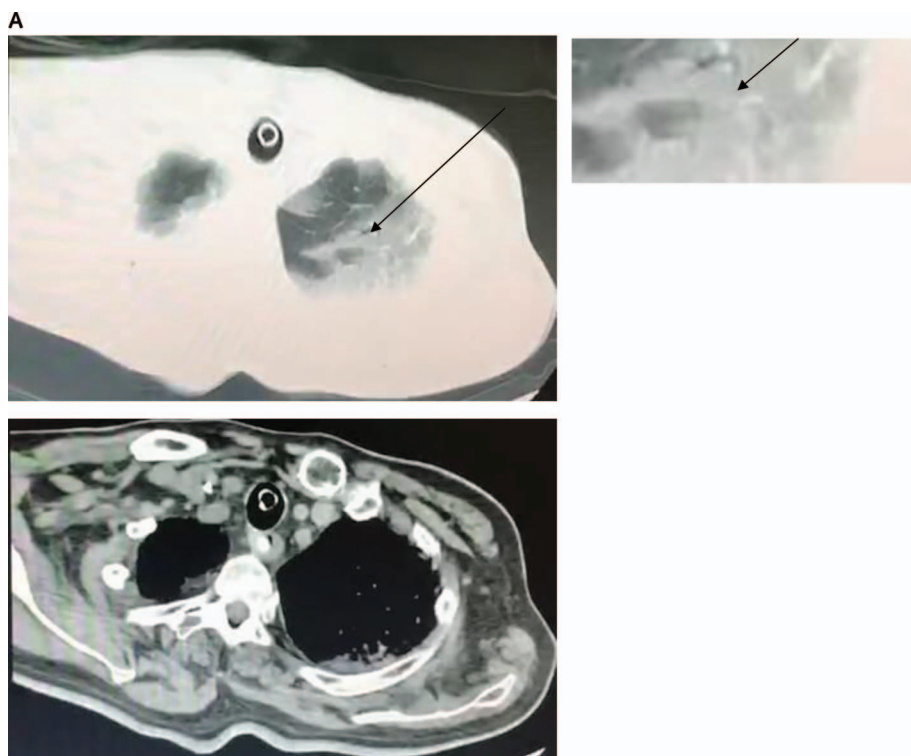
Biopsy lung sections were analyzed with hematoxylin-eosin staining, and immunostaining for SARS-CoV-2 was conducted as reported elsewhere (1). Throat swabs were assessed for SARS-CoV-2 by using real-time reverse transcriptase polymerase chain reaction assays (2).

The CT scans revealed patchy bilateral ground glass-like opacifications (Figure 1, A to C, arrows). Despite antiviral therapies, respiratory and hemodynamic instability continued and the patient died 3 weeks after diagnosis. Permission for post-mortem transthoracic needle biopsy, but not autopsy, was obtained from the patient's family.

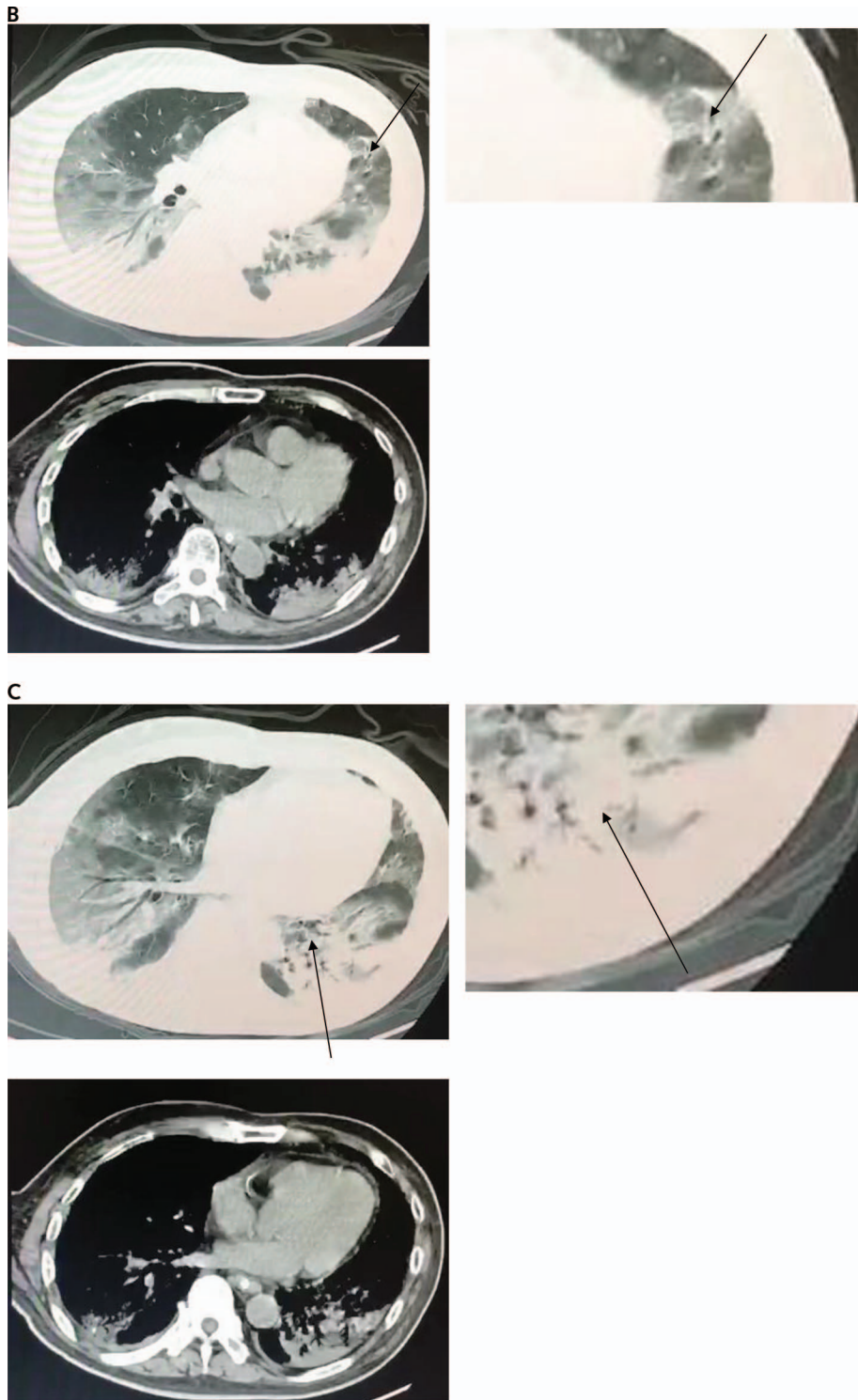
Histopathologic examination of lung biopsy tissues revealed diffuse alveolar damage, organizing phase. Denuded alveolar lining cells (Figure 2, A-1, arrow 1), with reactive type II pneumocyte hyperplasia, were noted (Figure 2, A-1, arrow 2). Intra-alveolar fibrinous exudates were present (Figure 2, A-2, arrow 3), along with loose interstitial fibrosis and chronic inflammatory infiltrates (Figure 2, A-2, arrow 4). Intra-alveolar loose fibrous plugs of organizing pneumonia were noted (Figure 2, A-3, arrow 5), with presence of intra-alveolar organizing fibrin seen in most foci (Figure 2, A-4, arrow 6).

Immunostaining of lung sections with an antibody to the Rp3 NP protein of SARS-CoV-2 revealed prominent expression on alveolar epithelial cells (Figure 2, B, top panel), including damaged, desquamated cells within the alveolar space

Figure 1. Computed tomographic images obtained from the patient 3 weeks after initial clinical manifestations of COVID-19 and 2 weeks before transthoracic biopsy, demonstrating ground glass-like opacifications.

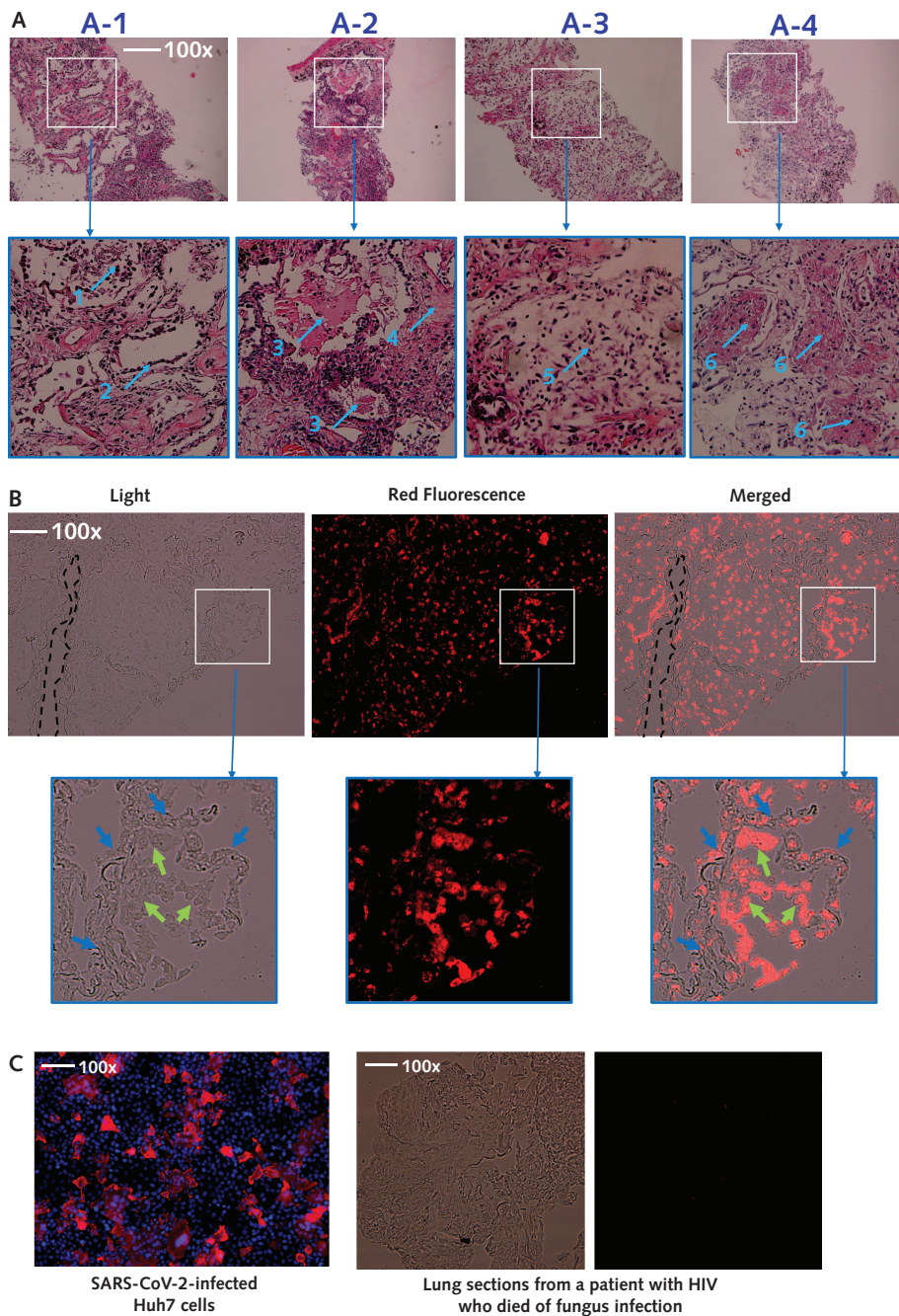


Continued on the following page

Figure 1—Continued.

Pleural thickening and enlarged mediastinal lymph nodes were present. Arrows indicate the approximate locations of the subsequently obtained postmortem transthoracic needle biopsy samples. A. Left upper anterior segment. B. Left upper lingular segment. C. Left lower lobe.

Figure 2. Histopathologic examination of lung biopsy tissues and immunostaining from a patient who died of COVID-19 ($\times 100$ magnification).



A. Histopathologic examination revealing diffuse alveolar damage, organizing phase (A-1); denudation of alveolar lining cells (*arrow 1*), with presence of reactive type II pneumocyte hyperplasia (*arrow 2*) (A-2); intra-alveolar fibrinous exudates (*arrow 3*) and interstitial loose fibrosis with chronic inflammatory infiltrates (*arrow 4*) (A-3); and intra-alveolar loose fibrous plugs (*arrow 5*) (A-4). In most foci, intra-alveolar organizing fibrin is seen (*arrow 6*). B. Immunostaining of SARS-CoV-2 in lung sections. Images were taken under light and fluorescent conditions, respectively ($\times 100$ magnification). Merged images were also generated. Blue arrows indicate interstitial areas between the alveoli, and green arrows indicate injured epithelial cells desquamated into the alveolar spaces. The dashed black lines indicate the blood vessel. Immunostaining of SARS-CoV-2 was done by using a rabbit polyclonal antibody (made in house, 1:100) against the Rp3 NP protein, which is highly conserved between SARS-CoV and SARS-CoV-2, followed by probing with a Cy3-conjugated goat antirabbit IgG (1:50, Abcam, ab6939). C. Positive and negative controls for immunostaining. For the positive control, the Huh7 cells were infected with SARS-CoV-2 at multiplicity of infection of 0.5 for 48 hours. After extensive washes, the cells were then fixed with 2.5% (wt/vol) glutaraldehyde. The infected cells were stained in red, and nuclei were stained with DAPI (Beyotime, Wuhan, China) in blue. For the negative control, biopsy lung sections derived from a patient with HIV who died of fungal infection were stained in parallel with lung sections from the patient with COVID-19 as above.

LETTERS

(Figure 2, B, bottom panel, green arrows). In contrast, viral protein expression was minimally detectable on blood vessels (Figure 2, B, dashed black line) or in the interstitial areas between alveoli (Figure 2, B, bottom panel, blue arrows). Immunostaining of Huh7 cells infected with SARS-CoV and of lung sections from an HIV-positive patient who died of fungal infection served as positive and negative staining controls, respectively (Figure 2, C).

Discussion: The histopathologic changes seen on post-mortem transthoracic needle biopsies from a patient with COVID-19 who had respiratory failure and radiographic bilateral ground-glass opacities are consistent with diffuse alveolar damage. Although such nonspecific findings may be seen in response to several conditions that result in respiratory failure, its demonstration in the setting of COVID-19 helps to inform the clinical course of disease.

Our study is limited by our inability to obtain larger tissue specimens. The present findings warrant further study with larger tissue samples, obtained by open or thoracoscopic lung biopsy, or autopsy, for example.

Huilan Zhang, PhD*

Center for Biomedical Research, NHC Key Laboratory of Respiratory Disease, Tongji Hospital, Tongji Medical College, Huazhong University of Science and Technology
Wuhan, China

Peng Zhou, PhD*

CAS Key Laboratory of Special Pathogens, Wuhan Institute of Virology, Center for Biosafety Mega-Science, Chinese Academy of Sciences
Wuhan, China

Yanqiu Wei, MD*

Huihui Yue, MD*

Yi Wang, PhD*

Center for Biomedical Research, NHC Key Laboratory of Respiratory Disease, Tongji Hospital, Tongji Medical College, Huazhong University of Science and Technology
Wuhan, China

Ming Hu, MD*

Wuhan Pulmonary Hospital

Wuhan, China

Shu Zhang, PhD

Center for Biomedical Research, NHC Key Laboratory of Respiratory Disease, Tongji Hospital, Tongji Medical College, Huazhong University of Science and Technology
Wuhan, China

Tanze Cao, MD

Pulmonary Hospital

Wuhan, China

Chengqing Yang, MD

Ming Li, MD

Guangyun Guo, MD

Xianxiang Chen, MD

Wuhan Pulmonary Hospital

Wuhan, China

Ying Chen, MD

CAS Key Laboratory of Special Pathogens, Wuhan Institute of Virology, Center for Biosafety Mega-Science, Chinese Academy of Sciences
Wuhan, China

Mei Lei, MD†

Institution of Tuberculosis for Prevention and Cure
Wuhan Pulmonary Hospital
Wuhan, China

Huiguo Liu, PhD†

Jianping Zhao, PhD†

Center for Biomedical Research, NHC Key Laboratory of Respiratory Disease, Tongji Hospital, Tongji Medical College, Huazhong University of Science and Technology
Wuhan, China

Peng Peng, MD†

Wuhan Pulmonary Hospital

Wuhan, China

Cong-Yi Wang, PhD†

Center for Biomedical Research, NHC Key Laboratory of Respiratory Disease, Tongji Hospital, Tongji Medical College, Huazhong University of Science and Technology
Wuhan, China

Ronghui Du, MD†

Wuhan Pulmonary Hospital

Wuhan, China

Note: Authors indicated with an asterisk (Drs. H. Zhang, P. Zhou, Y. Wei, H. Yue, Y. Wang, and M. Hu) contributed equally to this article. Authors indicated with a dagger (Drs. M. Lei, H. Liu, J. Zhao, P. Peng, C.-Y. Wang, and R. Du) served as co-senior authors.

Disclosures: Authors have disclosed no conflicts of interest. Forms can be viewed at www.acponline.org/authors/icmje/ConflictOfInterestForms.do?msNum=M20-0533.

Financial Support: By the National Natural Science Foundation of China (grants 81974456 and 91749207); the Clinical Research Physician Program of Tongji Medical College, Huazhong University of Science and Technology (grant 5001540075); and the SARS-CoV-2 Pneumonia Emergency Technology Public Relations Project (grants 2020FCA009 and 2020FCA026).

Correction: This article was corrected on 25 March 2020 to update author contributions.

doi:10.7326/M20-0533

References

1. Zhou P, Yang XL, Wang XG, et al. A pneumonia outbreak associated with a new coronavirus of probable bat origin. *Nature*. 2020. [PMID: 32015507] doi: 10.1038/s41586-020-2012-7
2. Corman VM, Landt O, Kaiser M, et al. Detection of 2019 novel coronavirus (2019-nCoV) by real-time RT-PCR. *Euro Surveill*. 2020;25. [PMID: 31992387] doi:10.2807/1560-7917.ES.2020.25.3.2000045